Adaptive White Point Extraction based on Dark Channel Prior for Automatic White Balance

Jieun Jo[1], Jaehyun Im[2], Jinbeum Jang[1], Yoonjong Yoo[3], and Joonki Paik[4]

[1] Image Processing and Intelligent Systems Laboratory, Department of Advanced Imaging, Graduate School of Advanced Imaging Science, Multimedia, and Film, Chung-Ang University, Seoul 06974, Korea
[2] CIS Division, SK Hynix Inc., Incheon-si, Gyeonggi-do 13558, Korea
[3] Vision Electronic Design Team, Hyundai Mobis Co., Ltd., Yongin-si, Gyeonggi-do 16891, Korea
[4] Image Processing and Intelligent Systems Laboratory, Department of Advanced Imaging, Graduate School of Advanced Imaging Science, Multimedia, and Film, Chung-Ang University, Seoul 06974, Korea   paikj@cau.ac.kr

* Corresponding Author: Joonki Paik

Abstract: This paper presents a novel automatic white balance (AWB) algorithm for consumer imaging devices. While existing AWB methods require reference white patches to correct color, the proposed method performs the AWB function using only an input image in two steps: i) white point detection, and ii) color constancy gain computation. Based on the dark channel prior assumption, a white point or region can be accurately extracted, because the intensity of a sufficiently bright achromatic region is higher than that of other regions in all color channels. In order to finally correct the color, the proposed method computes color constancy gain values based on the Y component in the XYZ color space. Experimental results show that the proposed method gives better color-corrected images than recent existing methods. Moreover, the proposed method is suitable for real-time implementation, since it does not need a frame memory for iterative optimization. As a result, it can be applied to various consumer imaging devices, including mobile phone cameras, compact digital cameras, and computational cameras with coded color.
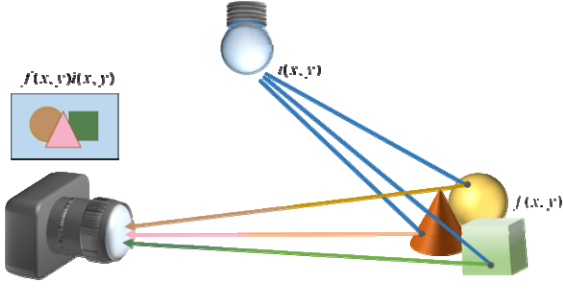
Keywords: Automatic white balance, Dark channel, White point estimation

1. Introduction

Color-correction techniques are important for many image processing-based applications, such as image retrieval, image classification, object recognition, object tracking, and registration [1-5]. While the human visual system is able to adapt to the color of the light source to recognize the true color of objects in a scene, the digital imaging sensor does not have a self-adaptation function [6-9]. Therefore, colored illumination results in color-biased measurements of an object toward the light source color [10-13]. Although the classical histogram equalization methods enhance contrast simply, they cannot adjust color distortion due to illumination temperature [14, 15]. In order to overcome this problem, digital cameras mimic the human color adaptation system using an automatic white balance (AWB) algorithm. The goal of the AWB algorithm is to provide color constancy with respect to illumination changes. In order to minimize user interaction in the AWB algorithm, the region that is similar to white color should automatically be detected [16].

Computationally efficient AWB methods have been proposed in the literature. Max-RGB is a fast, simple, color constancy algorithm that estimates the color of the light source from the maximum response among color channels [17]. The Gray-World hypothesis assumes that the average reflectance in the scene is achromatic [18]. In that original work, the hypothesis was used to determine that average reflectance for short-, middle-, and long-wave regions is the same. Another color constancy method is based on the gray edge hypothesis, which assumes that the average edge difference in the scene is achromatic [10, 19]. This method is based on the observation that the distribution of color derivatives exhibits the largest variation in the light source direction. The above-mentioned methods may fail if the color constancy

Fig. 1. The image acquisition model for the colored light source condition.

Fig. 2. Three test images with a color chart for the experiment (a) Indoor, (b) Pier, (c) Tiles.

Fig. 3. Block diagram of the proposed AWB method.

assumption is not satisfied when a set of colors per pixel significantly varies, depending on the scenes. To solve this problem, Im *et al.* proposed an AWB method based on dark channel prior [20], which estimates only one color constancy gain value. This method cannot avoid color distortion, since it applies the same gain value to all color channels. Dark channel prior was originally proposed for removing haze or fog in a scene by assuming that, in the most non-saturated regions of an image without haze or fog, at least one color channel has some pixels where intensities are very low and close to zero [21, 22]. In other words, it means that a white color or saturated region has very high intensity in all color channels. Therefore, a white region that is illuminated by a colored light source can be detected if the region has higher intensity pixels in all color channels than other regions.

This paper presents a robust AWB algorithm using dark channel prior without chromatic components. Although the proposed method uses dark channel prior, which was proposed by Im *et al.* [20], to detect the white point, it estimates each color constancy gain value by considering the Y component to correct red, green, and blue channels for better correction performance.

This paper is organized as follows. In Section 2, a novel image degradation model for color distortion is presented, and a white point detection method is presented in Section 3. Experimental results are given in Section 4, and Section 5 concludes the paper.

2. Theoretical background

In the original Retinex theory, a camera system acquires a color-distorted image that has all reflected lights in the field of view and the illumination. As shown in Fig. 1, the image sensor absorbs some colored light sources reflected from subjects that have original colors. So, the image acquisition model is defined as

$$g(x,y) = f(x,y) \cdot i(x,y), \qquad (1)$$

where $g(x,y)$ represents the acquired color-distorted input image acquired by the image sensor, $f(x,y)$ represents the input scene with reflected objects that have color vectors, and $i(x,y)$ is the illumination vector in each coordinate (x,y). Note that $i(x,y)$ has the same color
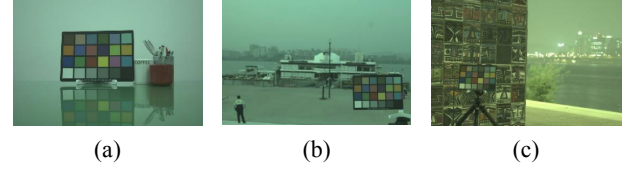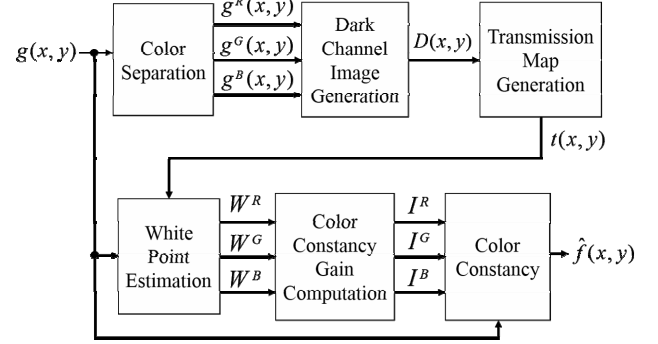
temperature since it represents the constant light source.

However, the color distortion problem is considered in the simple Retinex model. As shown in Fig. 2, the image sensor acquires some images with a strong specific color by color interpolation or the high sensitivity of the sensor [23]. Fortunately, illumination vector $i(x,y)$ is constant in (1), as mentioned above.

In order to perform white balancing from the color distorted version of $g(x,y)$ that has the color temperature of the illumination, we need to estimate the gray region from the input image. In this paper, we use dark channel prior to estimate it. He *et al.* proposed an image dehazing method using dark channel prior [21] as follows:

$$g(x,y) = f(x,y)t(x,y) + A \cdot \{1 - t(x,y)\}, \qquad (2)$$

where $t(x,y)$ represents the space-variant transmission coefficient that serves as the weighting factor in each pixel, and A is the atmospheric light. Although this image formation model is inspired by the foggy image formation model, we use only the colored illumination condition. So we assume A is a constant light source. In addition, $t(x,y)$ is generated to detect white points or regions in the proposed method using dark channel prior. Since most white points contain not only the pure white color but also saturated illumination components, the white and saturated regions can be differentiated based on a pre-specified threshold.

3. White Point Detection using Dark Channel Prior

As shown in Fig. 3, the proposed method detects the white point using a space-variant transmission map based
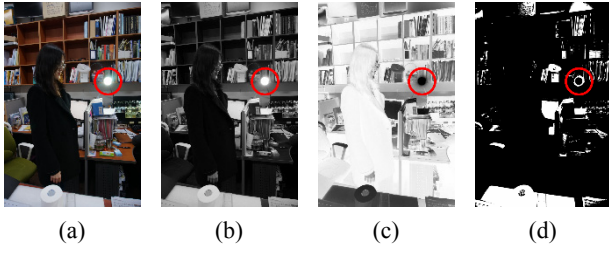
Fig. 4. White point detection based on dark channel prior (a) input color distorted image, (b) dark channel image, (c) space-variant transmission map, (d) detected white point regions.

on dark channel prior, and then computes the color constancy gain values. If the white point is accurately estimated, the corresponding computed color constancy gain values can accurately correct colors in the input distorted image. The modified dark channel prior is based on the observation that most local patches without a white light component contain some pixels where intensities are very low and close to zero in at least one color channel, as follows:

$$D(x,y) = \min_{c \in R,G,B} f^c(x,y) \approx 0 \qquad (3)$$

where $D(x,y)$ represents the dark channel image, and f^C represents one of the RGB color channels of f. According to this definition, the intensity of a white or saturated region is high in all the color channels.

The sequential result of the proposed white point estimation method is shown in Fig. 4. Saturated regions tend to have brighter pixels than other regions in the dark channel image, because each color channel has high intensity values, as shown in Fig. 4(b).

Although the dark channel image can provide a rough estimation of the white regions, accurate detection of the white region is not always possible, since it is difficult to differentiate the white region from others using only intensity values. For this reason, the proposed method generates the space-variant transmission map based on the dark channel image to accurately detect the white region, as follows:

$$t(x,y) = 1 - \frac{\min_c(g^c(x,y))}{A} + \frac{\min_c(f^c(x,y))}{A} \cdot t(x,y), \quad (4)$$

where $c \in R,G,B$, and A represents the constant light source, which can be defined as

$$A = \frac{1}{MN} \sum_{x=0}^{M} \sum_{y=0}^{N} \frac{R(x,y) + G(x,y) + B(x,y)}{3}, \qquad (5)$$

where M and N, respectively, represent the width and height of the input image.

If the light source contains a chromatic component, the white region cannot be detected in the observed image. In that case, the third term in (4) approaches zero, according to (5), and we have

$$t(x,y) = 1 - \frac{\min_c(g^c(x,y))}{A}, c \in \{R,G,B\}. \qquad (6)$$

Because the white or saturated region has high intensity and is close to 1 in the dark channel image, it appears darker in the transmission map, as shown in Fig. 4(c). As a result, the white point region can be detected using the transmission map by extracting the regions that have lower values than the average transmission coefficient, as follows:

$$P(x,y) = \begin{cases} 1, & \text{if } t(x,y) \leq \bar{t} \text{ and } f^c(x,y) < \theta \\ 0, & \text{otherwise} \end{cases}, \qquad (7)$$

where $C \in \{R,G,B\}$, P represents the binary image of white points, $\bar{t}$ is the average transmission coefficient, and θ is a threshold value to eliminate the saturated region. In the experiment, $\theta = 230$ is used to represent a value close to the maximum brightness. Because the intensity of the saturated region is very high in all color channels, it can be erroneously considered as a white region. To solve this problem, the proposed method eliminates the saturated region, as shown in Fig. 4(d). For instance, the region where the bulb is inside the lamp is not detected as a white region.

The detected region using Eq. (7) becomes a candidate white region, and its intensity in each color channel can be compute as

$$W^C = \frac{\sum\limits_{x,y \in \{P(x,y)=1\}} g^C(x,y)}{\sum\limits_{x,y \in \{P(x,y)=1\}} P(x,y)}, \text{ for } C \in \{R,G,B\}. \qquad (8)$$

To obtain accurate color constancy, chromatic components of the light source should be completely removed. In other words, each color channel has the same intensity value. In order to perform the color constancy algorithm, the proposed method computes luminance component Y in the XYZ color space by transforming W^C as follows:

$$Y = 0.2126 \cdot W^R + 0.7152 \cdot W^G + 0.0722 \cdot W^B. \qquad (9)$$

Because the color matching function is equal to the CIE standard photopic observer luminous efficiency curve, the Y component in the XYZ color space is suitable for the standard intensity [24]. Using the Y component, color constancy gains are computed as

$$I^C = \frac{W^Y}{W^C}, \text{ for } C \in \{R,G,B\} \qquad (10)$$

which are applied to the input image to estimate the color corrected image as

$$\hat{f}^C(x,y) = g^C(x,y) \cdot I^C, \text{ for } C \in \{R,G,B\}. \qquad (11)$$

(a)   (b)

(c)   (d)

(e)   (f)
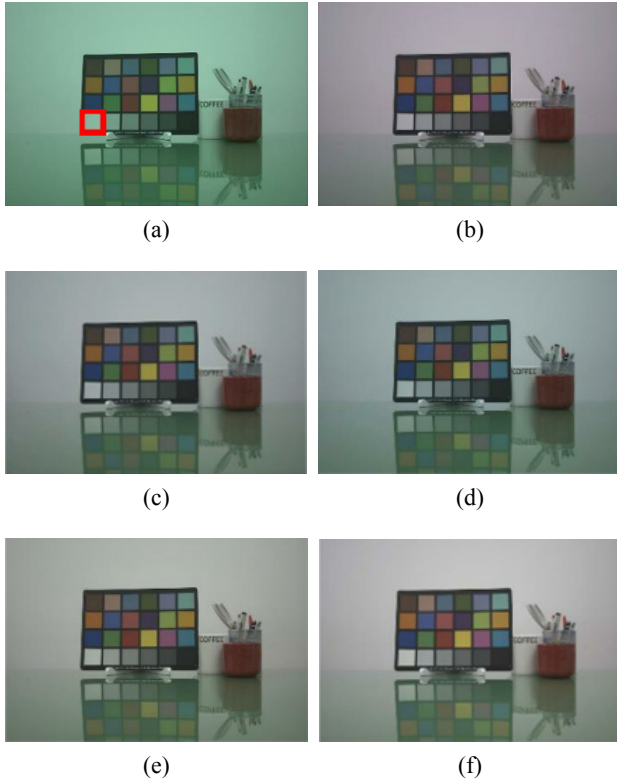
Fig. 5. Color-corrected results of the Indoor image using five different AWB methods (a) input raw image (the red box encloses the 19th patch in the color chart), (b) the result with Gray-World, (c) the result with Max-RGB, (d) the result from EWCC, (e) the result via the built-in AWB function, (f) the result using the proposed method.

4. Experimental Result

In the experiment, three test images at 1920×1280 are used, as shown in Fig. 2. These images were acquired using a digital single-lens reflex (DSLR) camera, and were recorded in raw format without using the built-in white balance function. Fig. 2(a) shows an indoor image, whereas Figs. 2(b) and 2(c) show outdoor images during the day and at night, respectively. These images contain a Macbeth color checker, which is the standard for estimating color conditions to test the degree to which image processes approximate the human visual system. In Fig. 5(a), the red box indicates the 19th patch of the Macbeth color checker, which appears white. The RGB value from this region is used to estimate the accuracy of white color representation. Performance by the proposed method was compared with four existing methods: i) Gray-World [18], ii) Max-RGB [17], iii) edge-weighting color constancy (EWCC) [10], and iv) the built-in AWB function of the commercial DSLR camera used in the experiment.

The color-corrected Indoor images using five different methods are shown in Fig. 5. All methods correct the color by suppressing green. Since Gray-World and EWCC methods insufficiently suppress the green and blue colors, the corresponding results look bluish, as shown in Figs.

Table 1. Numerical comparison of color errors of the 19th patch using the Indoor image.

Method	R	G	B	Error
Ground Truth	1.000	1.000	0.998	-
Input Image	1.000	1.327	1.173	0.3728
Gray-World	1.000	0.989	1.018	0.0253
Max-RGB	1.000	1.058	1.050	0.0796
EWCC	1.000	1.128	1.113	0.1738
System AWB	1.000	1.042	0.994	0.0418
Proposed Method	1.000	1.017	0.998	0.0168

5(b) and 5(c), respectively.

As shown in Figs. 5(d) and 5(e), Max-RGB and the built-in AWB method also insufficiently suppress the green and blue colors. On the other hand, the proposed method successfully suppresses the green and blue colors.

For a clearer comparison, the 19th patch of the color chart, which is enclosed by the red box shown in Fig. 5(a), is used. Although the ground truth of the red, green, and blue components of the patch is (243,243,242), the input color-distorted image gives different values [25]. The color error between the ground truth and color-corrected values can be computed as

$$E = \sqrt{(R_t \cdot R_c)^2 + (G_t \cdot G_c)^2 + (B_t \cdot B_c)^2}, \qquad (12)$$

where subscripts t and c, respectively, represent the ground truth and color-corrected values. Table 1 shows the numerical comparison of the five AWB methods. Because the input image has higher green and blue components than the ground truth, the cyan color dominates the entire image. The proposed method successfully suppresses the green and blue colors close to the ground truth values, while the other four methods exhibit larger color errors.

Results of the color-corrected Pier image are shown in Fig. 6. As shown in Figs. 6(c) and 6(d), the Max-RGB and EWCC methods produce bluish results, whereas the other methods successfully correct the color.

As shown in Table 2, Max-RGB and EWCC produce large color errors because of insufficient suppression of the green and blue colors. On the other hand, Gray-World, the built-in AWB, and the proposed methods perform successful color correction in the sense of color error.

Results of the color-corrected Tiles image are shown in Fig. 7, and their numerical comparison is given in Table 3. Blue and green colors of the corrected results using Gray-World and EWCC methods are still higher than the red color, and the corresponding results look bluish, as shown in Figs. 7(b) and 7(d). The input image is dominated by a green color, as shown in Fig. 7(a), and the result from Max-RGB is also greenish, as shown in Fig. 7(c), since it considers the maximum intensity region (which is green) to be white. The numerical error from the Max-RGB method is the same as that of the input distorted image, which coincides with subjective observation. On the other hand, the built-in AWB function over-suppresses the green and blue colors, and the corresponding result turns reddish, as shown in Fig. 7(e). The proposed method produces the
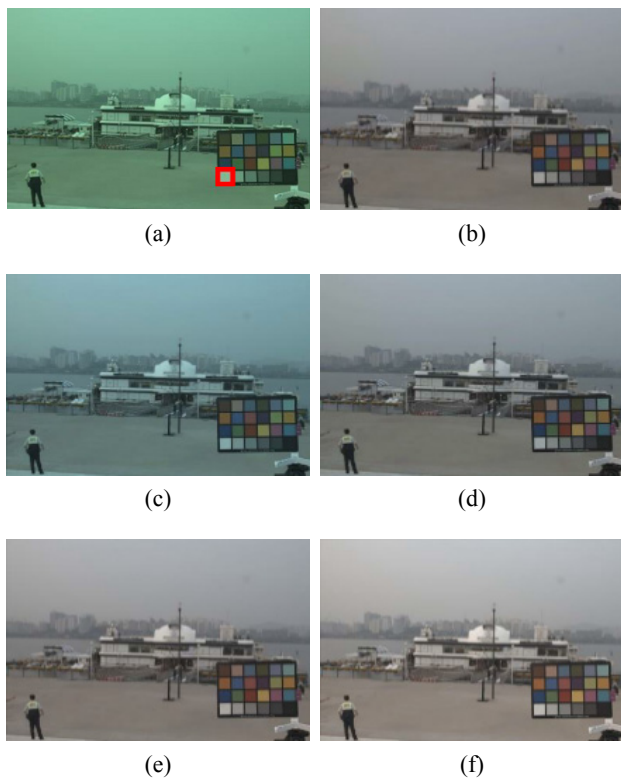
(a)   (b)

(c)   (d)

(e)   (f)

Fig. 6. Color-corrected results of the Tiles image using five different AWB methods (a) input raw image (the red box encloses the 19th patch in the color chart), (b) the result with Gray-World, (c) the result with Max-RGB, (d) the result from EWCC, (e) the result via the built-in AWB function, (f) the result from the proposed method.

(a)   (b)

(c)   (d)

(e)   (f)

Fig. 7. Color-corrected results of the Tiles image using five different AWB methods (a) input raw image (the red box encloses the 19th patch in the color chart), (b) the result with Gray-World, (c) the result with Max-RGB, (d) the result from EWCC, (e) the result via the built-in AWB function, (f) the result from the proposed method.
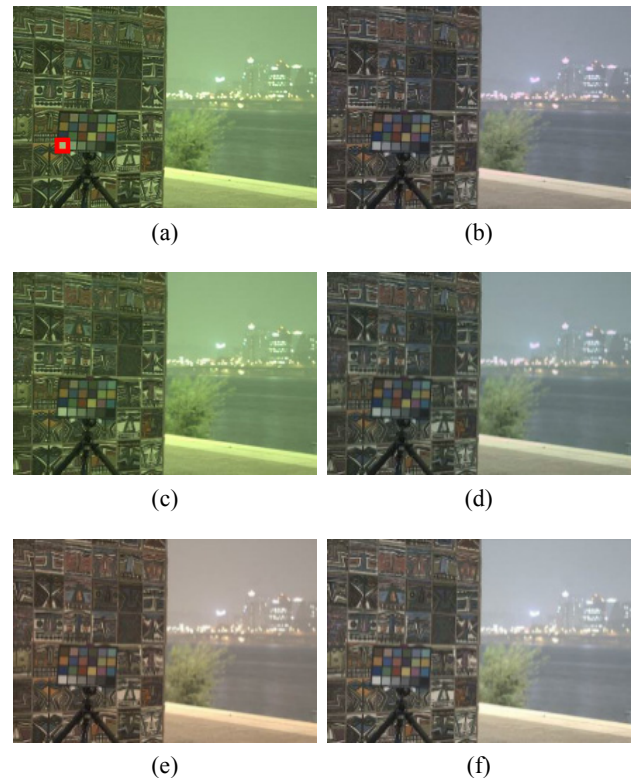
Table 2. Numerical comparison of color errors of the 19th patch using the Pier image acquired under daylight.

Method	R	G	B	Error
Ground Truth	1.000	1.000	0.998	-
Input Image	1.000	1.426	1.172	0.4612
Gray-World	1.000	0.998	0.980	0.0152
Max-RGB	1.000	1.257	1.256	0.3668
EWCC	1.000	1.084	1.051	0.1012
System AWB	1.000	0.989	0.967	0.0299
Proposed Method	1.000	1.009	1.007	0.0148

Table 3. Numerical comparison of color errors of the 19th patch using the Tiles image acquired at night.

Method	R	G	B	Error
Ground Truth	1.000	1.000	0.998	-
Input Image	1.000	1.189	0.805	0.2681
Gray-World	1.000	1.010	1.014	0.0217
Max-RGB	1.000	1.189	0.805	0.2681
EWCC	1.000	1.085	1.024	0.0898
System AWB	1.000	0.915	0.830	0.1858
Proposed Method	1.000	1.002	0.985	0.0148

best results in terms of both objective and subjective measures.

5. Conclusion

Since the proposed AWB method does not use the existing assumption that the average reflectance in the real world is achromatic, it can avoid excessive suppression of the dominant color, which is the main reason for incomplete color correction. More specifically, the proposed method accurately detects the white point using

dark channel prior based on the novel image degradation model for color distortion. Because the white point is an achromatic region, it has similar intensity in all three color channels, and higher intensity than other color regions in a dark channel image. For this reason, the proposed method can accurately detect the white point and compute the color constancy gain values. In the experiment, the proposed method corrects the color distortion better than existing methods. Therefore, the proposed method can be applied to various consumer digital imaging devices and computational cameras based on color coding [26, 27].

Acknowledgement

References

[1] T. Gevers and A. Smeulders, "Color based object recognition," *Pattern Recognition*, vol. 32, no. 3, pp. 453-464, March 1999. Article (CrossRef Link)

[2] K. Barnard, L. Martin, A. Coath, and B. Funt, "A comparison of computational color constancy algorithms-part II: Experiments with image data," *IEEE Trans. Image Processing*. Vol. 11, no. 9, pp. 985-996, September 2002. Article (CrossRefLink)

[3] J. Renno, D. Makris, T. Ellis, and G. Jones, "Application and evaluation of colour constancy in visual surveillance," *Proc. 2nd IEEE International Workshop on Visual Surveillance and Performance Evaluation of Tracking and Surveillance*, pp. 301-308, October 2005. Article (CrossRefLink)

[4] Y. Kim, S. Jeong, J. Oh, and S. Lee, "Fast MOG (mixture of gaussian) algorithm based on predicting model parameters," *TechArt: Journal of Arts and Imaging Science*, vol. 2, no. 1, pp. 41-45, February 2015. Article (CrossRefLink)

[5] S. Lee, S. Jeong, H. Yu, G. Kim, H. Kwak, E. Kang, and S. Lee, "Efficient image transformation and camera registration for the multi-projector image calibration," *TechArt: Journal of Arts and Imaging Science*, vol. 3, no. 1, pp. 38-42, February 2016. Article (CrossRefLink)

[6] B. Zhang and A. Batur, "A real-time auto white balance algorithm for mobile phone cameras," *Proc. IEEE International Conference on Consumer Electronics*, pp. 1-4, 2012. Article (CrossRefLink)

[7] J. Im, J. Jeon, M. Hayes, and J. Paik, "Single image-based ghost-free high dynamic range imaging using local histogram stretching and spatially adaptive denoising," *IEEE Transactions on Consumer Electronics*, vol. 57, no. 4, pp. 1478-1484, November 2011. Article (CrossRefLink)

[8] J. Im, S. Lee, and J. Paik, "Improved elastic registration for removing ghost artifacts in high dynamic imaging," *IEEE Transactions on Consumer Electronics*, vol. 57, no. 2, pp. 932-935, May 2011. Article (CrossRefLink)

[9] S. Lee, D. Zhang, and S. Ko, "Image contrast enhancement based on a multi-cue histogram," *IEIE Transactions on Smart Processing and Computing*, vol. 4, no. 5, pp. 349-353, October 2015. Article (CrossRefLink)

[10] A. Gijsenij, T. Gevers, and J. Weijer, "Improving color constancy by photometric edge weighting," *IEEE Transactions on Pattern Analysis and Machine Intelligence*, vol. 34, no. 5, pp. 918-929, May 2012. Article (CrossRefLink)

[11] R. Charrière, M. Hébert, A. Trémeau, and N. Destouches, "Color calibration of an RGB camera mounted in front of a microscope with strong color distortion," *Applied Optics*, vol. 52, no. 21, pp. 5262-5271, July 2013. Article (CrossRefLink)

[12] N. Baniˊc and S. Lonˇcariˊc, "Smart light random memory sprays retinex: a fast retinex implementation for high-quality brightness adjustment and color correction," *Journal of the Optical Society of America A*, vol. 32, no. 11, pp. 2136-2147, November 2015. Article (CrossRefLink)

[13] A. Gijsenij, T. Gevers, and M. P. Lucassen, "Perceptual analysis of distance measures for color constancy algorithms," *Journal of the Optical Society of America A*, vol. 26, no. 10, pp. 2243-2256, October 2009. Article (CrossRefLink)

[14] J. Im and J. Paik, "Spatially adaptive histogram equalization for single image-based ghost-free high dynamic range imaging," *TechArt: Journal of Arts and Imaging Science*, vol. 1, no. 1, pp. 55-59, February 2014. Article (CrossRefLink)

[15] S. Jung, "Exact histogram specification considering the just noticeable difference," *IEIE Transactions on Smart Processing & Computing*, vol.3, no.2, pp. 52-58, April 2014. Article (CrossRefLink)

[16] R. Lukac, "Refined automatic white balancing," *Electronics Letters*, vol. 43, no. 8, pp. 445-446, April 2007. Article (CrossRefLink)

[17] E. Land, "The retinex theory of color vision," *Scientific American*, vol. 237, no. 6, pp. 108-128, December 1977. Article (CrossRefLink)

[18] G. Buchsbaum, "A spatial processor model for object colour perception," *Journal of the Franklin Institute*, vol. 310, no. 1, pp. 1-26 , July 1980. Article (CrossRefLink)

[19] J. Weijer, T. Gevers, and A. Gijsenij, "Edge-based color constancy," *IEEE Transactions on Image Processing*, vol. 16, no. 9, pp. 2207-2214, September 2007. Article (CrossRefLink)

[20] J. Im, D. Kim, J. Jung, T. Kim, and J. Paik, "Dark channel prior-based white point estimation for automatic white balance," Proc. IEEE International Conference on Consumer Electronics, pp. 127-128, January 2014. Article (CrossRefLink)

[21] K. He, J. Sun, and X. Tang, "Single image haze removal using dark channel prior," *IEEE Transactions on Pattern Analysis and Machine Intelligence*, vol. 33, no. 12, pp. 2341-2353, December 2011. Article (CrossRefLink)

[22] C. Yeh, L. Kang, M. Lee, and C. Lin, "Haze effect removal from image via haze density estimation in optical model," *Optics Express*, vol. 21, no. 22, pp. 27127-27141, November 2013. Article (CrossRefLink)

[23] D. Cheng, D. K. Parasad, and M. S. Brown, "Illuminant estimation for color constancy: why spatial-domain methods work and the role of the

color distribution," *Journal of the Optical Society of America A*, vol. 31, no. 5, pp. 1049-1058, March 2014. Article (CrossRefLink)

[24] E. Reinhard, G. Ward, S. Pattanaik, P. Debevec, W. Heidrich, K. Myszkowki, "High Dynamic Range Imaging: Acqusistion, Display, and Image-based Lighting, 2nd Edition," Morgan Kaufmann, 2010. Article (CrossRefLink)

[25] C. S. McCamy, H. Marcus, and J. G. Davidson, "A Color-Rendition Chart". Journal of Applied Photographic Engineering, vol. 2, no. 3, pp. 95-99, 1976. Article (CrossRefLink)

[26] S. Kim, E. Lee, M. Hayes, and J. Paik, "Multifocusing and depth estimation using a color shift model-based computational camera," *IEEE Transaction Image Processing*, vol. 21, no. 9, pp. 4152-4166, September 2012. Article (CrossRefLink)

[27] S. Lee, M. Hayes, and J. Paik, "Distance estimation using a single computational camera with dual off-axis color filtered apertures," *Optics Express*, vol. 21, no. 20, pp. 23116-23129, October 2013. Article (CrossRefLink)

Jieun Jo was born in Yeongcheon, Korea, in 1991. She received a BSc in electricity and electronic engineering from Ulsan University in 2015. she is pursuing an MSc in digital imaging at Chung-Ang University. Her research interests include image enhancement, stereo vision, and seam estimation.

Jaehyun Im was born in Seoul, Korea, in 1984. He received a BSc in electronic engineering from Kang-nam University, Korea, in 2007. He received an MSc and a PhD in image engineering from Chung-Ang University, Seoul, Korea, in 2009 and 2012. Currently, he is working at SK Hynix. His research interests include image restoration, image enhancement, digital auto-focusing, image and video processing, and real-time object tracking.

Jinbeum Jang was born in Suwon, Korea, in 1989. He received a BSc in digital media from Sang-Myung University, Korea, in 2014. Also, he graduated with an MSc in image science from Chung-Ang University, Korea, in 2016. Currently, he is pursuing a PhD in image science at Chung-Ang University. His research interests include image enhancement, auto focusing, and depth generation.

Yoonjong Yoo was born in Seoul, Korea, in 1981. He received a BSc in electronic engineering from Chung-Ang University, Seoul, Korea, in 2005. He received an MSc in image engineering from Chung-Ang University, Seoul, Korea, in 2007. From 2009 to 2013, he worked at Nextchip, where he designed auto-exposure, auto-white-balance, and wide-dynamic-range functions for surveillance cameras. He received a PhD in image processing from Chung-Ang University, Seoul, Korea, in 2015. Currently, he is working at Hyundae Mobis. His research interests include image enhancement and restoration for display processing, video compression standards, and surveillance video applications.

Joonki Paik was born in Seoul, Korea, in 1960. He received a BSc in control and instrumentation engineering from Seoul National University in 1984. He received an MSc and a PhD in electrical engineering and computer science, respectively, from North-western University in 1987 and 1990, respectively. From 1990 to 1993, he worked at Samsung Electronics, where he designed image stabilization chip sets for consumer camcorders. Since 1993, he has been on the faculty at Chung-Ang University, Seoul, Korea, where he is currently a professor in the Graduate School of Advanced Imaging Science, Multimedia, and Film. From 1999 to 2002, he was a visiting professor in the Department of Electrical and Computer Engineering at the University of Tennessee, Knoxville. Dr. Paik was a recipient of the Chester Sall Award from the IEEE Consumer Electronics Society, the Academic Award from the Institute of Electronic Engineers of Korea, and the Best Research Professor Award from Chung-Ang University. He has served the IEEE Consumer Electronics Society as a member of the editorial board. Since 2005, he has been the head of the National Research Laboratory in the field of image processing and intelligent systems. In 2008, he worked as a full-time technical consultant for the System LSI Division at Samsung Electronics, where he developed various computational photographic techniques, including an extended depth-of-field (EDoF) system. From 2005 to 2007, he served as Dean of the Graduate School of Advanced Imaging Science, Multimedia, and Film. From 2005 to 2007, he was Director of the Seoul Future Contents Convergence (SFCC) Cluster established by the Seoul Research and Business Development (R&BD) Program. Dr. Paik is currently serving as a member of the Presidential Advisory Board for Scientific/Technical Policy for the Korean government, and is a technical consultant for the Korean Supreme Prosecutor's Office for computational forensics.